engineering proceedings

MDPI

*Proceeding Paper*

# Design, Construction, and Initial Testing of a Transportable Mobile Energy Station with Autonomous Solar Tracking †

**Armand Pellja, Tormi Lillerand, Indrek Virro, Yevhen Ihnatiev, Olga Liivapuu * and Jüri Olt**

Chair of Biosystems Engineering, Institute of Forestry and Engineering, Estonian University of Life Sciences, F. R. Kreutzwaldi 56/1, 51006 Tartu, Estonia; armand.pellja@emu.ee (A.P.); tormi.lillerand@emu.ee (T.L.); indrek.virro@emu.ee (I.V.); yevhen.ihnatiev@emu.ee (Y.I.); jyri.olt@emu.ee (J.O.)

* Correspondence: olga.liivapuu@emu.ee

† Presented at the 1st International Online Conference on Inventions—Energy Security and Sustainable Development, 25–26 June 2026; Available online: https://sciforum.net/event/IOCIV2026.

**Abstract**

A road-transportable hybrid energy station was designed, assembled, and commissioned for isolated and emergency loads. The platform integrates 6.82 kWp photovoltaics on four foldable actuator-positioned faces and a roof, 14.4 kWh lithium iron phosphate storage, three 8 kVA single-phase inverters configured for three-phase output, an LPG generator, and distributed Siemens control. During a cloudy 6 °C outdoor electric vehicle test, the station supplied a three-phase EV load for 1 h 15 min. The original test record reports 13.9 kWh, although the energy measurement method was not documented. The representative point combined 1.554 kW photovoltaic input with 10.269 kW battery discharge against an 11.073 kW charging load. The results demonstrate deployable three-phase service while identifying precharge, conductor heating, storage capacity, and tracking validation requirements.

**Keywords:** photovoltaics; lithium iron phosphate storage; electric vehicle charging; programmable logic control; rural electrification; emergency resilience

## 1. Introduction

Electricity access becomes an energy security problem when a site is remote, temporary, connected to a weak and unreliable grid or exposed to disruption. Contemporary rural electrification research therefore treats local generation, storage, and demand as a coordinated system rather than as isolated devices [1,2]. A transportable source adds a further requirement: the complete plant must comply with road transport constraints, deploy quickly, and supply useful loads without permanent civil works. Such systems may be particularly relevant to agricultural operations, temporary field sites, and emergency response applications.

Recent photovoltaic system reviews emphasize that reliable autonomous operation depends on matching generation, conversion, storage, and control at the architecture level [3]. Energy storage is particularly important because photovoltaic production and load demand rarely coincide. In the present system, lithium iron phosphate batteries were selected because of their cycle life, thermal stability, and suitability for controlled operation in a compact mobile installation [4].

For a mobile platform, the resulting design problem is constrained simultaneously by mass, enclosure volume, current carrying capacity, phase configuration, monitoring, and backup availability. An apparently sufficient sum of component ratings can still fail in

Check for updates

Academic Editor: Said Al-Hallaj

Published: 27 November 2026

**Copyright:** © 2026 by the authors. Licensee MDPI, Basel, Switzerland. This article is an open access article distributed under the terms and conditions of the Creative Commons Attribution (CC BY) license.

practice if precharge, conductor temperature, phase order, or communication compatibility is neglected.

Solar tracking can increase the irradiation captured by a photovoltaic surface, but reviews show that gains depend on axis arrangement, tracking accuracy, shading, the energy consumed by the tracking mechanism and weather [5,6]. Mechanical protection and the ability to stow photovoltaic modules under adverse weather conditions are important design considerations for movable photovoltaic structures [7]. In the present prototype, these requirements are particularly relevant because the movable photovoltaic surfaces also form part of the trailer enclosure during transport. A mobile tracker must therefore balance energy capture with stiffness, synchronized motion, fail-safe stowage, and maintenance. This tradeoff differs from a fixed ground array because every actuator, hinge, cable, and sensor also affects legal transport dimensions and deployment reliability.

Electric vehicle charging provides a demanding field load through which such an architecture can be tested. Charging station studies increasingly combine photovoltaic generation, batteries, and supervisory control to reduce dependence on upstream infrastructure [8]. Standalone solar charging reviews nevertheless show that storage size and operating policy dominate service continuity whenever irradiation is limited [9]. Multi-objective studies further demonstrate that photovoltaic and battery capacities cannot be selected independently of charger demand and connection mode [10]. Proceedings work on off-grid sizing reaches the same conclusion: an apparently small load or resource change can alter the required array and storage configuration [11].

At the distribution-network level, coordinated planning of EV charging demand, renewable generation, and battery energy storage can reduce the adverse effects of charging loads under variable generation and demand conditions [12].

Although numerous studies address the sizing and optimization of hybrid renewable energy systems, fewer publications provide detailed experimental results for fully implemented mobile systems. A recent mobile energy station for emergency supply in rural and isolated areas integrated 2.88 kW of flexible photovoltaic modules, a 19.2 kWh $LiFePO_4$ battery bank, a 5 kW inverter–charger, and a 4 kW generator on an all-terrain pickup truck [13]. That system was evaluated over ten months using a simulated rural medical-post load. The present prototype differs in its use of a road trailer with foldable photovoltaic surfaces, 6.82 kWp of installed PV capacity, a 14.4 kWh battery bank, three-inverter power conversion for three-phase AC output, and distributed programmable motion control. However, experimental information on the commissioning and initial operation of such road-transportable three-phase hybrid energy systems remains limited. The recent literature follows two main research directions. Solar-tracking studies focus on positioning accuracy, mechanical reliability, and measured energy gain [5–7,14–16]. PV-battery and EV studies mainly address component dimensioning, energy management, and charging schedules [8–11,13,17–20]. Many of these studies focus on simulations or stationary systems. Experimental evidence from complete transportable mobile energy station systems remains limited.

The aim of this study was to document the design and commissioning of a road-transportable hybrid energy station and to conduct a preliminary functional evaluation of its three-phase power delivery capability during an outdoor electric vehicle charging session. The specific objectives were to (1) describe the implemented photovoltaic, storage, power conversion, protection, and control architecture; (2) document the implementation of the distributed solar-positioning control; (3) identify the principal integration problems encountered during commissioning and the corresponding corrective actions; and (4) report the energy transferred during one outdoor charging session and compare the available PV, battery, and EV charging power readings at a representative operating point.

https://doi.org/10.3390/engproc2026152028

## 2. Materials and Methods

### *2.1. Prototype Architecture and Component Configuration*

The Tiki CP600 trailer has a 3500 kg gross rating. Its architecture couples local generation, battery storage, and a controllable vehicle load. Photovoltaic and battery capacities were selected jointly because they are interdependent under variable resource and demand [14]. Electrical schematics were prepared in CADMATIC 2021 Electrical; settings and observations came from the hardware and Victron Remote Management interface.

The array contains twenty-two SunMan SMF310M-5X12DW_p modules rated at 310 Wp. Module data are $V_{mp} = 33.3$ V and $I_{mp} = 9.31$ A at maximum power, $V_{oc} = 40.5$ V open-circuit, and $I_{sc} = 9.81$ A short-circuit. The total installed PV capacity and the voltage, current and power ratings of each series–parallel group from Table 1 were calculated using Equation (1).

$$P_{PV,rated} = 22(310\ W) = 6.82\ kW,$$
$$V_{oc,g} = n_s V_{oc,m}, \qquad I_{sc,g} = n_p I_{sc,m}. \tag{1}$$

**Table 1.** Defining Equation (1) symbols.

| Symbol | Meaning | Unit/Note |
|---|---|---|
| $P_{PV,rated}$ | Total rated peak power of the photovoltaic system | kWp |
| $V_{oc,g}$ | Open-circuit voltage of PV group g | V |
| $n_s$ | Number of PV modules connected in series | Number of modules |
| $V_{oc,m}$ | Open-circuit voltage of one PV module | V |
| $I_{sc,g}$ | Short-circuit current of PV group g | A |
| $n_p$ | Number of parallel-connected PV strings | Number of strings |
| $I_{sc,m}$ | Short-circuit current of one PV module | A |

Each 3S2P long wing gives 121.5 V open-circuit, 19.62 A short-circuit, and 1.86 kWp. The ten-module 2S5P roof and end group gives 81.0 V, 49.05 A, and 3.10 kWp. These values reconcile all twenty-two modules and correct an eight-module intermediate thesis calculation. Each orientation group feeds one SmartSolar MPPT 150/70 VE.Can controller [11].

Figure 1 shows the commissioned trailer in transport and operating configurations together with the principal internal power hardware. The physical evidence is important because mobile station studies often remain at the sizing or simulation stage [11,12].

The images confirm installation of the complete power and control chain. They do not demonstrate tracking accuracy or energy gain, which require controlled measurements.

Three 4.8 kWh $LiFePO_4$ battery modules connected in parallel form a 48 V-class, 14.4 kWh nominal battery bank. Two Lynx Distributor units connect the battery bank, three MPPT charge-controller outputs, and three Quattro 48/8000/100 inverter–chargers. One inverter–charger is assigned to each phase to form the three-phase AC output. A detachable LPG GE-7000T generator is connected to the AC input as a backup source. Cerbo GX provides system monitoring and records available VE.Can, VE.Bus, and battery data through the VRM platform. Table 2 summarizes the implemented power and communication connections. Figure 2 maps these relationships.

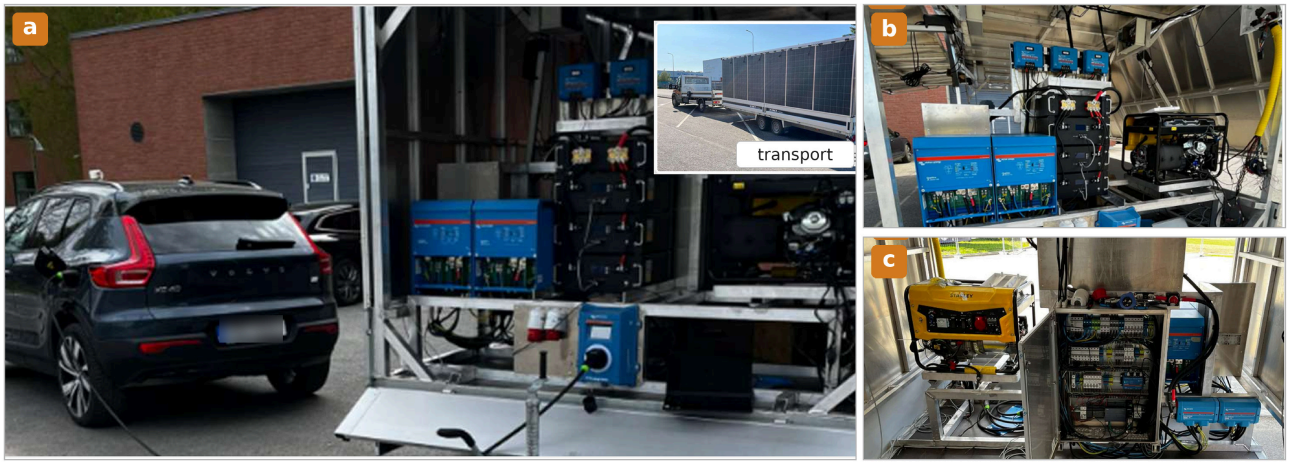



**Figure 1.** Commissioned transportable energy station: (**a**) outdoor electric vehicle charging with the transport configuration inset; (**b**) inverter, storage and charge control installation; (**c**) LPG generator, distribution cabinet and monitoring equipment.

**Table 2.** Principal ratings and implemented subsystem configuration.

| Subsystem | Implemented Configuration | Rating or Setting |
|---|---|---|
| Transport platform | Tiki CP600 road trailer | Maximum permissible gross mass: 3500 kg |
| PV array and grouping | 22 × 310 W; 3S2P, 3S2P and 2S5P | 6.82 kWp; groups 1.86, 1.86 and 3.10 kWp |
| Charge control | 3 × SmartSolar MPPT 150/70 VE.Can | 150 V input class; 70 A output class |
| Storage | 3 × 4.8 kWh $LiFePO_4$ modules in parallel | 48 V class; 14.4 kWh nominal |
| AC conversion | 3 × Quattro 48/8000/100; one per phase | 3 × 8 kVA nominal |
| Backup | LPG GE-7000T generator | 7.5 kW stated; 10% start and 70% stop SoC |
| Automation and monitoring | S7-1215C; 4 × LOGO! 8; 6 × LA36; Cerbo GX | 24 V actuators; 0 to 10 V feedback; VRM records |

The generator enters the AC side, whereas PV and battery meet at the DC bus. Consequently, the DC source readings and AC vehicle load do not share an identical measurement boundary [14].

Figure 3 visualizes the control system architecture, feedback, and communication paths. The diagram distinguishes ordinary control functions from the still unvalidated safety and synchronization functions [15,16].

### *2.2. Solar-Positioning and Distributed Control*

The S7-1215C calculated solar elevation from day number, local time, latitude, declination, and hour angle using Equation (2) of the source thesis and the Siemens LGF astronomical-clock functions. Coordinates 58.378025° N and 26.728493° E were used for testing in Tartu. The S7 transmitted target and direction commands over Modbus TCP to four local LOGO! 8 controllers. Each LOGO! controller read one 0–10 V actuator-position channel, scaled it to 0–700 mm, and switched actuator relays until feedback entered a

±3-unit deadband around the target. The 0–10 V signal represented 0 to 700 mm stroke. Mapping 700 mm to 135° gives Equation (2).

$$k_l = \frac{\Delta l}{\Delta \theta} = \frac{700\ \text{mm}}{135^\circ} = 5.19\ \text{mm}/^\circ \quad (2)$$

This is only an average linear mapping; it was not a calibrated geometric linkage model. Therefore, no tracking-accuracy or energy-gain claim is made. The long sides used two actuators driven by a common command, but only one position-feedback channel, so actuator skew could not be detected. Six frame-mounted travel switches indicated that the PC surface had reached the folded position. Two emergency-stop buttons were connected to standard Siemens S7 digital inputs and stopped the actuators through PLC logic. No safety-rated controller was used, and the emergency-stop function was not validated against machinery operating-safety standards.

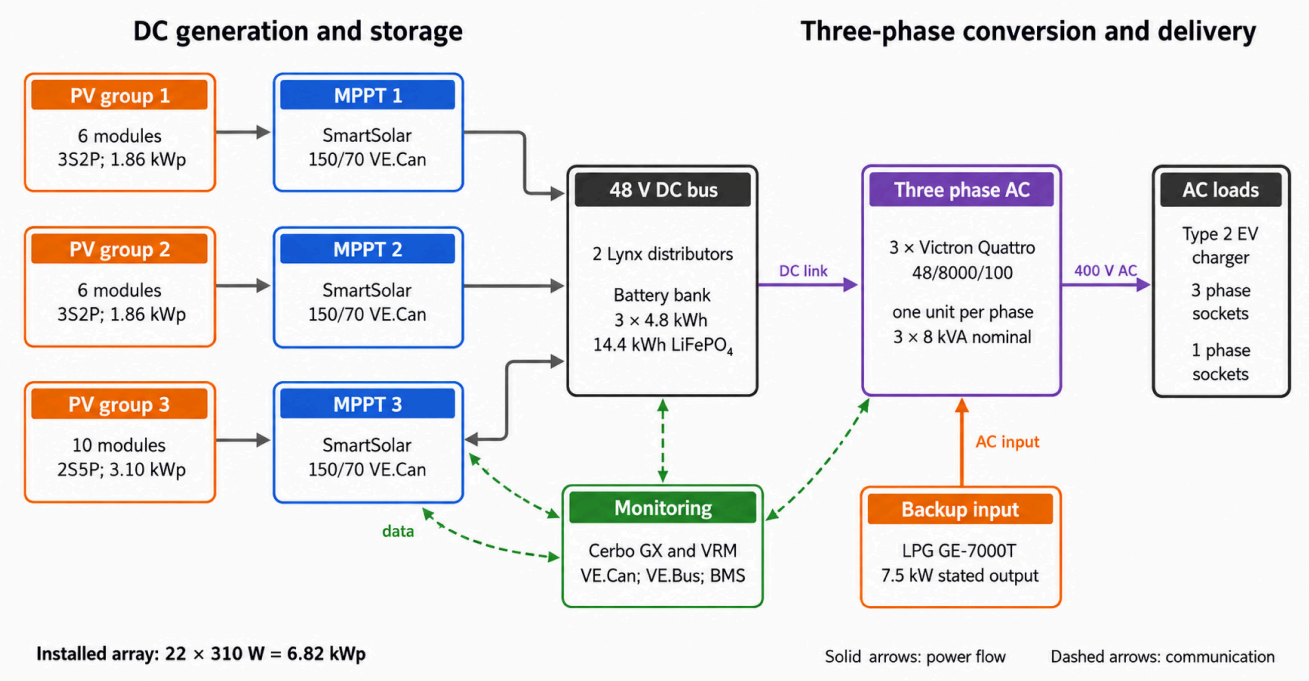



**Figure 2.** Implemented electrical architecture. Solid lines show power flow; dashed lines show data paths. Three inverter–chargers form the three-phase output.

### *2.3. Commissioning and Outdoor EV Charging Test*

Commissioning used staged energization: batteries, inverter–chargers, PV MCB isolators, main distribution protection, and local cabinet protection were energized sequentially while checking for alarms and protective-device operation. Initial direct battery connection caused a BMS short-circuit alarm attributed to inverter DC-link inrush. A workshop 72 Ω resistor was temporarily connected between the battery negative terminal and inverter negative cable; DC-link voltage was monitored with a multimeter before the resistor was bypassed and the inverters were energized. The resistor power rating, exact connection duration, target voltage, multimeter model, and acceptance criterion were not recorded. The procedure is reported only as a commissioning observation and not as a validated or reproducible precharge method.

The outdoor EV charging test was conducted in the Estonian University of Life Sciences parking area using a three-phase Type 2 connection. The weather was cloudy and the ambient temperature was 6 °C with cloudy weather. The long PV wings remained folded, while the short sides were positioned parallel to the ground. The station battery state of charge was 99% at the beginning of the test. Charging started at 6 A and ended at 16 A.

The vehicle model, verified battery capacity, vehicle state of charge, station final state of charge, intermediate current settings, and the timing of the current changes were not recorded. The test is treated as a preliminary functional charging test rather than a reproducible vehicle-specific performance test.

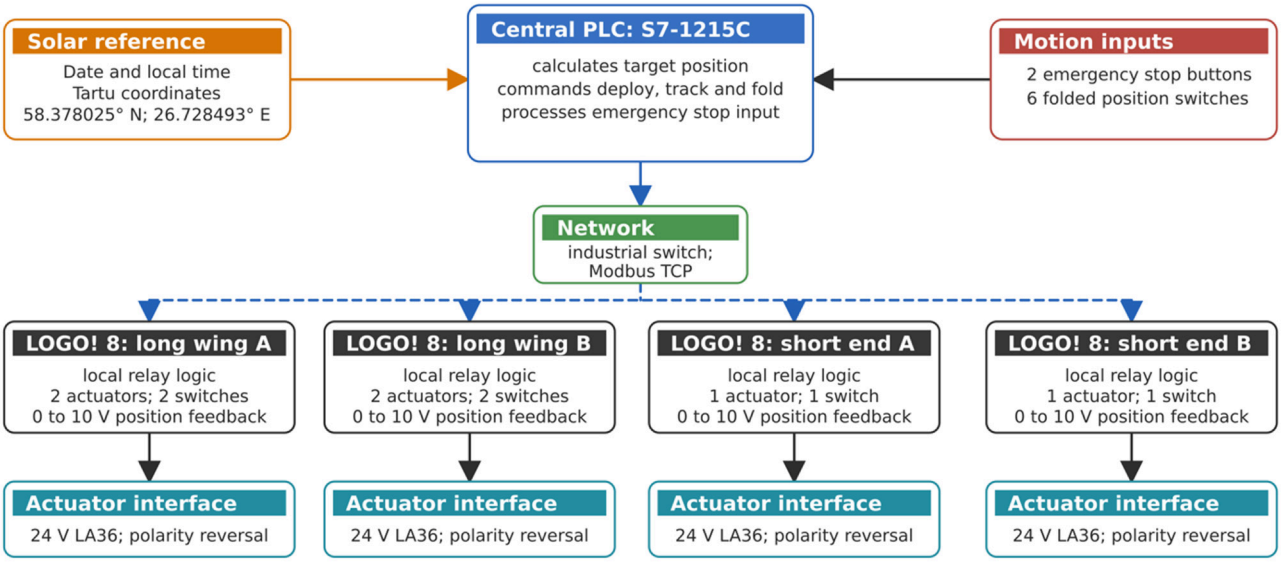



**Figure 3.** Distributed solar-positioning control. The S7-1215C commands four LOGO! 8 actuator interfaces through Modbus TCP.

## 3. Results

### *3.1. Realization and Commissioning*

The project progressed to a road-transportable prototype containing the complete power and control chain. Four photovoltaic bearing body faces serve as the vertical enclosure and become positioned collectors after deployment; the roof remains fixed. This geometry implements the foldable four-face architecture disclosed in published Estonian patent application EE 202300003 A, while the individual PV, battery, generator, and monitoring components remain established [7]. The application is not a granted patent and does not attribute inventorship to the article author.

Cerbo GX established monitoring; three MPPTs communicated through VE.Can; the inverter–chargers formed a three-phase VE.Bus set; and the S7 exchanged commands with four LOGO! 8 units. Wing commands and feedback were observed [15]. No target angle, measured angle, tracking error, or fixed reference series was recorded, so tracking gain and accuracy remain unverified [17].

Four local control cabinets were selected in the design phase to place the LOGO! 8 I/O and relay interfaces near the actuators, while the S7-1215C retained the central solar-position calculation. The Siemens S7 logic controller retains central calculation. Successful communication alone cannot establish tracking performance [15].

Commissioning identified four practical issues. Direct inverter connection triggered a battery-management fault. Temporary precharging through a 72 Ω resistor allowed the inverters to be connected without repeating the fault, but the procedure was not documented for reproduction. AC charging then required phases 1 and 3 to be exchanged, and battery communication required a type B rather than type A CAN cable. Finally, the original battery conductors heated strongly with an apparent discrepancy near 1.2 kW. Replacement corrected the practical concern, but the data do not isolate conductor loss from conversion and auxiliary demand.

After correction, staged energization caused no reported protection trip. The result demonstrates backup logic, not generator reliability. Table 3 separates observations, settings, and verification needs.

**Table 3.** Commissioning and field results, evidence type, and remaining verification need.

| Observation | Quantitative Evidence and Status | Interpretation and Next Verification |
|---|---|---|
| Inverter startup | 72 Ω DC-link precharge; observed | Rate the circuit; verify voltage and time |
| AC and data interfaces | phases 1 and 3 exchanged; type B CAN; observed | Check phase sequence and connector type |
| High current wiring | heating and about 1.2 kW apparent gap; observed | Measure resistance, temperature and boundary loss |
| Outdoor EV session | 13.9 kWh in 1.25 h; 11.12 kW average | Repeat across weather and state of charge |
| Displayed power values | 1.554 kW PV; 10.269 kW battery; 11.073 kW EV | Repeat using synchronized DC and AC measurements |
| Tracking and backup | position logic; 10% to 70% rule; configured | Measure error, gain, skew and endurance |

### *3.2. Outdoor Electric Vehicle Charging*

The EV was charged through a Type 2 connection using three-phase AC. At one operating point, the Victron VRM display showed 1.554 kW of PV input, 10.269 kW of battery discharge, and 11.073 kW of EV charging power. The original test record reports 13.9 kWh over 1 h 15 min. The meter type, calibration status, measurement boundary, and energy-integration method were not documented. Figure 4 avoids forcing these values into an ideal balance because charging depends on simultaneous renewable, storage, and load conditions [18].

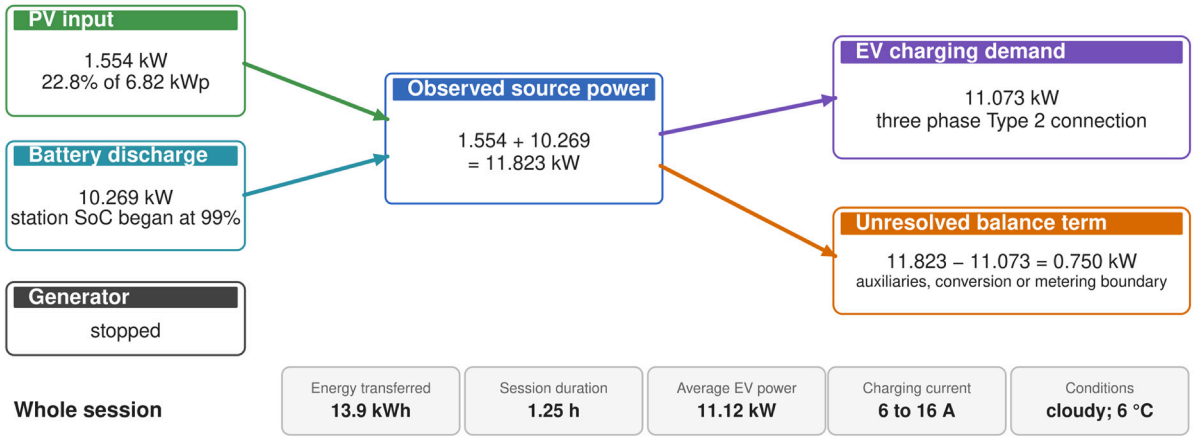



**Figure 4.** Displayed power values during the outdoor EV charging test. The values were not confirmed to have identical timestamps or measurement boundaries.

While measuring, the PV, battery, and EV power values were 1.554 kW, 10.269 kW and 11.073 kW. The readings were not confirmed to have identical timestamps for the defined measurement boundaries and therefore were presented separately. No system efficiency or complete power balance was calculated from measured values.

The whole session provides a consistency check. Equation (3) gives 11.12 kW average EV power, only 0.047 kW or 0.42% above the 11.073 kW display. This supports the load magnitude, not the DC-to-AC balance [18].

$$\overline{P}_{\mathrm{EV}} = \frac{E_{\mathrm{EV}}}{t} = \frac{13.9\ \mathrm{kWh}}{1.25\ \mathrm{h}} = 11.12\ \mathrm{kW}. \quad (3)$$

During the outdoor test, the displayed instantaneous PV power was 1.554 kW under cloudy conditions, while the long PV wings remained folded. This measurement reflects the PV output only under the specific conditions at the time of observation and does not describe the system's efficiency, capacity factor, utilization factor, or overall energy yield. The vehicle model, battery capacity, initial and final state of charge, and energy transferred to the vehicle were not recorded. Therefore, the available test data cannot be used to determine the energy required for a specified charging range or the corresponding EV charging duration.

The verified outcome is practical three-phase delivery, not optimized renewable charging. Stored energy and limited concurrent PV met the load with the generator off. The 14.4 kWh bank suits partial charging and shorter loads, not an unsupported 30 kWh vehicle increment [10,18].

## 4. Discussion

The closest prototype used 2.88 kW PV, 19.2 kWh storage, a 5 kW inverter, and a 4 kW gasoline generator [13]. The present station has 2.37 times the PV rating, three 8 kVA units, tracked body faces, and outdoor EV charging. Its battery is 25% smaller, and the comparator ran for ten months [12]. This work is stronger for three-phase architecture but weaker for longitudinal reliability, so overall superiority is not claimed.

The present test confirmed the operation of the positioning control but did not measure tracking accuracy or energy gain. A controlled comparison between tracked and fixed PV modules requires synchronized measurements of panel angle, irradiance, power, energy, temperature, and actuator consumption. This comparison is planned for the next suitable summer measurement period. Additional testing could not be completed during the revision period because seasonal peak PV production was already declining.

The field test clarifies the storage constraint. Even at an 11.12 kW average vehicle load, the installed battery contains only about 1.30 h of nominal energy before conversion losses and reserve limits are considered. Predictive battery scheduling could allocate this limited buffer more deliberately under uncertain renewable input [19]. Generator start at 10% state of charge and stop at 70% were configured, but no low state endurance cycle was observed [2]. Generation forecasting could also decide when to restrict charging, deploy the wings, or start backup generation [20]. Such upgrades should follow synchronized metering; otherwise, a more complex controller would optimize around the unresolved 0.750 kW boundary error.

Three safety points remain critical. The MPPT voltage check must include the module temperature coefficient and winter minimum. Paired long wing actuators need independent skew detection. Emergency stop and restart need a safety relay or controller, risk assessment, and manual reset before unattended use [7,17]. These steps separate a functioning prototype from transferable field technology. Formal safety validation was outside the scope of the commissioning tests. A risk assessment matrix is required.

## 5. Conclusions

The 3500 kg trailer integrates 6.82 kWp PV, 14.4 kWh storage, 24 kVA conversion, and a 7.5 kW LPG source.

The preliminary EV test lasted 1 h 15 min. The original test record reports 13.9 kWh of charging energy. The measurement method and meter traceability were not documented.

The 11.073 kW EV load coincided with 1.554 kW PV, 10.269 kW battery discharge, and a 0.750 kW unresolved residual.

Commissioning identified the need for temporary DC-link precharging, phase correction, a correct CAN cable, and replacement of the original battery conductors. The precharge and safety functions require further validation.

Actuator mapping was 5.19 mm per degree; tracking, skew, and generator endurance remain unquantified.

**Author Contributions:** Conceptualization O.L. and J.O., methodology T.L., software I.V., validation Y.I. and T.L., analysis O.L. and A.P., investigation I.V. and T.L., data curation Y.I., T.L. and I.V., visualization A.P. and T.L., writing, and approval A.P., O.L. and J.O. All authors have read and agreed to the published version of the manuscript.

**Funding:** Prototype development was conducted within P250159MIBT.

**Data Availability Statement:** Available upon request from the corresponding author.

**Conflicts of Interest:** The authors declare no conflicts of interest.

## References

1. Silinto, B.F.; van der Laag Yamu, C.; Zuidema, C.; Faaij, A.P.C. Hybrid renewable energy systems for rural electrification in developing countries: A review on energy system models and spatial explicit modelling tools. *Renew. Sustain. Energy Rev.* **2025**, *207*, 114916. [CrossRef]
2. Taghizad-Tavana, K.; Esmaeel Nezhad, A.; Hagh, M.T.; Canani, A.; Safari, A. Hybrid Renewable Energy Systems for Off-Grid Electrification: A Comprehensive Review of Storage Technologies, Metaheuristic Optimization Approaches and Key Challenges. *Eng* **2025**, *6*, 309. [CrossRef]
3. Motamedisedeh, O.; Omrani, S.; Karim, A.; Drogemuller, R.; Walker, G. A comprehensive review of optimum integration of photovoltaic-based energy systems. *Renew. Sustain. Energy Rev.* **2025**, *207*, 114935. [CrossRef]
4. Ngoy, K.R.; Lukong, V.T.; Yoro, K.O.; Makambo, J.B.; Chukwuati, N.C.; Ibegbulam, C.; Eterigho-Ikelegbe, O.; Ukoba, K.; Jen, T.-C. Lithium-ion batteries and the future of sustainable energy: A comprehensive review. *Renew. Sustain. Energy Rev.* **2025**, *223*, 115971. [CrossRef]
5. Paliyal, P.S.; Mondal, S.; Layek, S.; Kuchhal, P.; Pandey, J.K. Automatic solar tracking system: A review pertaining to advancements and challenges in the current scenario. *Clean Energy* **2024**, *8*, 237–262. [CrossRef]
6. Kumba, K.; Upender, P.; Buduma, P.; Sarkar, M.; Simon, S.P.; Gundu, V. Solar tracking systems: Advancements, challenges, and future directions: A review. *Energy Rep.* **2024**, *12*, 3566–3583. [CrossRef]
7. Buchroithner, A.; Visser, L.; Preßmair, R.; McClone, G.; Kleissl, J. The future of PV tracking? An interdisciplinary performance assessment of a novel design with panel protection. *Renew. Sustain. Energy Rev.* **2025**, *212*, 115287. [CrossRef]
8. Ghanbari Motlagh, S.; Oladigbolu, J.; Li, L. A review on electric vehicle charging station operation considering market dynamics and grid interaction. *Appl. Energy* **2025**, *392*, 126058. [CrossRef]
9. Oruganti, K.S.P.; Vaithilingam, C.A.; Kumaresh, S.S.; Ramasamy, A.; Happonen, A. An integrative review of standalone solar powered EV charging stations: Standards, policies, design aspects, and future directions. *Energy Rep.* **2025**, *14*, 2893–2913. [CrossRef]
10. Gönül, Ö.; Duman, A.C.; Güler, Ö. Multi-objective optimal sizing and techno-economic analysis of on- and off-grid hybrid renewable energy systems for EV charging stations. *Sustain. Cities Soc.* **2024**, *115*, 105846. [CrossRef]
11. Guamangallo, J.; Porras, J.; Quinatoa, C.; Vaca, J.; Chiza, L. Optimal Sizing of Hybrid Generation Systems (Photovoltaic System and Energy Storage System) for Off-Grid Applications. *Eng. Proc.* **2024**, *77*, 24. [CrossRef]
12. Balu, K.; Mukherjee, V. Optimal deployment of electric vehicle charging stations, renewable distributed generation with battery energy storage and distribution static compensator in radial distribution network considering uncertainties of load and generation. *Appl. Energy* **2024**, *359*, 122707. [CrossRef]
13. Milón Guzmán, J.J.; Braga, S.L.; Pradelle, F.A.Y.; Díaz Coa, M.E.; Infa Mamani, C.K. Experimental Evaluation of a Mobile Charging Station Prototype for Energy Supply Applied to Rural and Isolated Areas in Emergency Situations. *Energies* **2025**, *18*, 465. [CrossRef]
14. Pirayawaraporn, A.; Sappaniran, S.; Nooraksa, S.; Prommai, C.; Chindakham, N.; Jamroen, C. Innovative sensorless dual-axis solar tracking system using particle filter. *Appl. Energy* **2023**, *338*, 120946. [CrossRef]

15. Aggarwal, A.; Himanshu, H.; Sidana, M.; Gupta, G.; Sodhi, I.S.; Sharma, A. Efficiency Enhancement and Estimation of Photovoltaic Energy Generation Using Dual-Axis Tracking Systems. *Eng. Proc.* **2025**, *95*, 4. [CrossRef]
16. Sadeghi, R.; Parenti, M.; Memme, S.; Fossa, M.; Morchio, S. A Review and Comparative Analysis of Solar Tracking Systems. *Energies* **2025**, *18*, 2553. [CrossRef]
17. Laksahapsoro, B.; Bird, M.; Acha, S.; Shah, N. Optimisation of photovoltaic and battery systems for cost-effective energy solutions in commercial buildings. *Appl. Energy* **2025**, *392*, 125907. [CrossRef]
18. Rehman, A.U.; Lu, J.; Du, B.; Bai, F.; Sanjari, M.J. Efficient Management of Electric Vehicle Charging Stations: Balancing user preferences and grid demands with energy storage systems and renewable energy. *Appl. Energy* **2025**, *393*, 126147. [CrossRef]
19. Rezaeimozafar, M.; Duffy, M.; Monaghan, R.F.D.; Barrett, E. Residential PV-battery scheduling with stochastic optimization and neural network-driven scenario generation. *Energy Rep.* **2024**, *12*, 418–429. [CrossRef]
20. Chaaban, A.K.; Alfadl, N. A comparative study of machine learning approaches for an accurate predictive modeling of solar energy generation. *Energy Rep.* **2024**, *12*, 1293–1302, Correction in *Energy Rep.* **2024**, *12*, 5960. https://doi.org/10.1016/j.egyr.2024.11.083. [CrossRef]

**Disclaimer/Publisher's Note:** The statements, opinions and data contained in all publications are solely those of the individual author(s) and contributor(s) and not of MDPI and/or the editor(s). MDPI and/or the editor(s) disclaim responsibility for any injury to people or property resulting from any ideas, methods, instructions or products referred to in the content.